Journal of Thermal Analysis and Calorimetry, Vol. 90 (2007) 1, 93–97

NANOSCALE SPINEL FERRITES PREPARED BY MECHANOCHEMICAL ROUTE
Thermal stability and size dependent magnetic properties

V. Šepelák[1,2,3*], *P. Heitjans*[2,4] *and K. D. Becker*[1,2]

[1]Institute of Physical and Theoretical Chemistry, Braunschweig University of Technology, Hans-Sommer-Strasse 10 38106 Braunschweig, Germany
[2]Center for Solid State Chemistry and New Materials, Leibniz University of Hannover, Callinstrasse 3-3A 30167 Hannover, Germany
[3]Institute of Geotechnics, Slovak Academy of Sciences, Watsonova 45, 04353 Košice, Slovakia
[4]Institute of Physical Chemistry and Electrochemistry, Leibniz University of Hannover, Callinstrasse 3-3A 30167 Hannover, Germany

Among the many types of preparation and processing techniques, the nonconventional mechanochemical route has been recognized as a powerful method for the production of novel, high-performance, and low-cost nanomaterials. Because of their small constituent sizes and disordered structural state, nanoscale materials prepared by mechanochemical route are inherently unstable with respect to structural changes at elevated temperatures. Taking into account the considerable relevance of the thermal stability of nanoscale complex oxides to nanoscience and nanotechnology, in the present work, results on the response of mechanochemically prepared $MgFe_2O_4$ and $NiFe_2O_4$ to changes in temperature will be presented. Several interesting features are involved in the work, e.g., a relaxation of the mechanically induced cation distribution towards its equilibrium configuration, a disappearance of the superparamagnetism on heating, an increase of both the saturation magnetization and the Néel temperature with increasing particle size, and a core–shell structure of nanoparticles.

Keywords: *ferrite, mechanochemistry, Mössbauer spectroscopy, nanomaterial, thermogravimetry*

Introduction

Interest in nanosized spinel ferrites of the type MFe_2O_4 (M is a divalent metal cation) has greatly increased in the past few years due to their importance in understanding the fundamentals in nanomagnetism [1] and their wide range of applications including high-density data storage, ferrofluid technology, sensor technology, spintronics, magnetocaloric refrigeration, heterogeneous catalysis, magnetically guided drug delivery, magnetic resonance imaging [2–5]. To emphasize the site occupancy at the atomic level, the structural formula of 2–3 spinel ferrites may be written as $(M^{2+}_{1-\lambda}Fe^{3+}_{\lambda})[M^{2+}_{\lambda}Fe^{3+}_{2-\lambda}]O_4$, where parentheses and square brackets denote cation sites of tetrahedral (A) and octahedral [B] coordination, respectively. λ represents the so-called degree of inversion defined as the fraction of the (A) sites occupied by Fe^{3+} cations.

At present, the high-energy milling method is widely used for the preparation of nanostructured materials due to its relative simplicity and availability [6]. This method can deliver nanocrystalline spinel ferrites (and oxides in general) either by particle size reduction of bulk material to the nanometer scale without changes in its chemical composition [7–9] or by inducing a heterogeneous solid-state chemical reaction between the ferrite precursors, i.e., by the mechanically induced formation reaction (mechanosynthesis) [10–21]. Nanoscale spinel ferrites prepared by mechanochemical route are often inherently unstable owing to their small constituent sizes, non-equilibrium cation distribution, disordered spin configuration, and high chemical activity [21]. Subsequent thermal treatment of mechanochemically prepared spinel ferrites causes their transition from an excited metastable state into a low-energy crystalline state. During the process of annealing, the advantageous properties of the nanosized spinel ferrites are mostly lost [22], thus an understanding of the thermal stability of nanostructure and of the relaxation mechanism of mechanically induced metastable states is necessary. A better understanding of the response of nanoscale spinel ferrites to changes in temperature is crucial not only for basic science but also because of their possible high-temperature applications [23].

To gain insight into the thermal stability and relaxation of the mechanically induced disorder, the

* Author for correspondence: v.sepelak@tu-bs.de

1388–6150/$20.00

Akadémiai Kiadó, Budapest, Hungary
Springer, Dordrecht, The Netherlands

present work focuses on the study of the response of mechanochemically prepared $MgFe_2O_4$ and $NiFe_2O_4$ nanoparticles to changes in temperature.

Experimental

Nanocrystalline $MgFe_2O_4$ and $NiFe_2O_4$ with an average particle size of about 9.6 and 8.6 nm were prepared by high-energy milling coarse powders of high-purity $MgFe_2O_4$ and by mechanochemical synthesis from binary oxide precursors (NiO, α-Fe_2O_3), respectively, as reported in our earlier work [8, 24, 25]. In the present study, $MgFe_2O_4$ and $NiFe_2O_4$ samples are annealed at various temperatures up to 1280 K in air to investigate their thermal stability and magnetic evolution with grain growth process.

The Néel temperature (T_N) was determined using a thermogravimetric (TG) analyzer (Setaram Tag 24 thermobalance) equipped with a permanent magnet. Nanocrystalline $MgFe_2O_4$ (130 mg) was annealed at four consecutive temperatures (1130, 1180, 1230, 1280 K) in open platinum crucibles without removing it from the TG analyzer. The sample was held at the given annealing temperature for 2 h, cooled to 470 K at a cooling rate of 10 K min^{-1}, and then heated to the further annealing temperature. The magnetic disorder–order transition of the sample in the magnetic field of the permanent magnet was monitored during the cooling stage. T_N was arbitrarily defined by the maximum slope of the curve. The upper baseline of the curve corresponded to the true sample mass. Reproducibility of the measured T_N was ±0.5 K.

Mössbauer spectra were taken in transmission geometry using a ^{57}Co/Rh γ-ray source. The velocity scale was calibrated relative to ^{57}Fe in Rh. Recoil spectral analysis software [26] was used for the quantitative evaluation of the Mössbauer spectra. The degree of inversion, λ, was calculated from the Mössbauer subspectral intensities $I_{(A)}/I_{[B]}=(f_{(A)}/f_{[B]})[\lambda/(2-\lambda)]$, assuming that the ratio of the recoilless fractions is $f_{[B]}/f_{(A)}=0.94$ at room temperature [27].

Magnetic measurements were made using a SQUID magnetometer. The average particle size of the annealed samples was determined by XRD using the PowderCell program [28] and by TEM (JOEL JEM-2100F).

Results and discussion

Relaxation of nonequilibrium cation distribution in nanocrystalline spinel ferrite

The most remarkable effect in spinel ferrites is the strong dependence of properties on the state of structural disorder and, in particular, on the cation distribution. This is clearly documented in the case of $MgFe_2O_4$, whose Néel temperature, T_N, was found to be a sensitive function of the degree of inversion, λ, and has been used by several authors as a means of characterizing the cation distribution of $MgFe_2O_4$ samples. For example, O'Neill *et al*. [29] performed the differential scanning calorimetric measurements to show that T_N of $MgFe_2O_4$ increases linearly with increasing λ. It should be noted that these authors used a quenching procedure to obtain various degrees of inversion in the bulk $MgFe_2O_4$ samples by freezing-in their high-temperature cation distributions.

Taking into account that T_N provides a readily observed, highly sensitive measure of cation distribution in $MgFe_2O_4$, we have also measured this quantity for the high-energy milled and subsequently annealed (at four various temperatures) $MgFe_2O_4$ sample, so as to obtain information on the particle size dependent cation distribution in the material. In the present case, T_N was determined using TG measurements (Fig. 1), where the apparent mass of the $MgFe_2O_4$ sample in the magnetic field of the permanent magnet was recorded as a function of temperature. It is clearly visible from both thermogravimetric and derivate thermogravimetric curves that the apparent mass of the

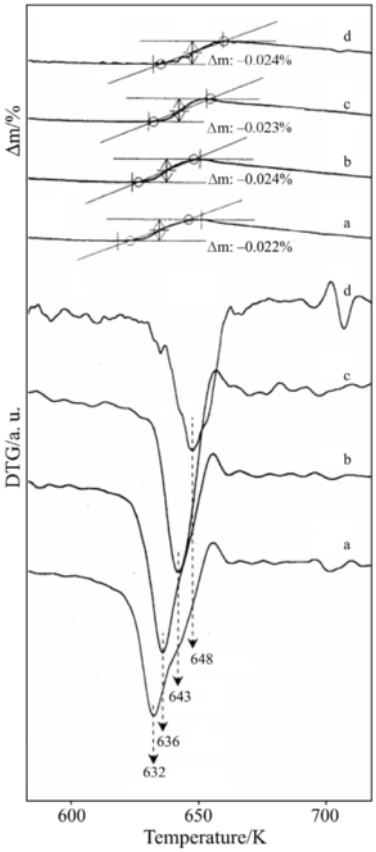

Fig. 1 TG and DTG curves for the high-energy milled $MgFe_2O_4$ after consecutive annealing at a – 1130, b – 1180, c – 1230 and d – 1280 K

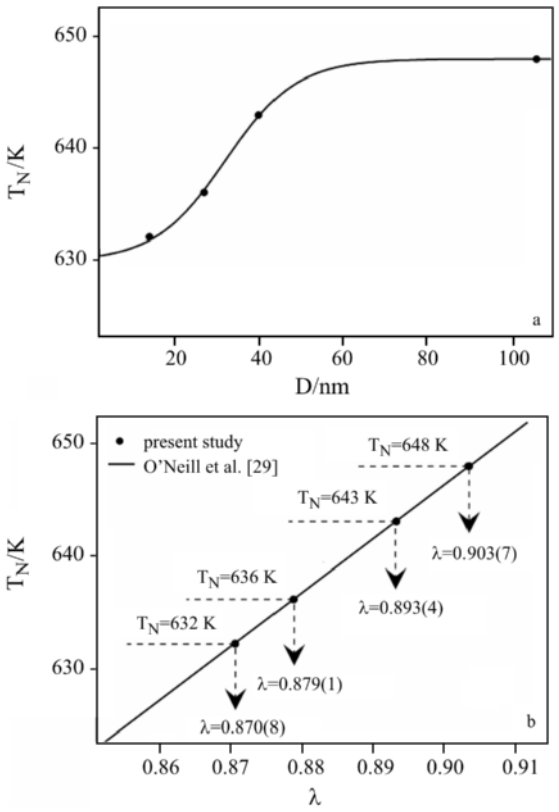

Fig. 2 Néel temperature, T_N, *vs*. a – the particle size, D and b – the degree of inversion, λ, for the high-energy milled and subsequently annealed $MgFe_2O_4$ sample. (Solid line is guide to eye.) The linear increase of T_N with increasing λ is plotted from [29] in Fig. 2b (straight line)

sample decreased rapidly due to loss of spontaneous magnetization, when the sample passed through T_N. The important observation is that T_N of the sample increases with increasing annealing temperature, i.e., with increasing particle size. The estimated T_N values of 632, 636, 643 and 648 K characterize the magnetic transition in $MgFe_2O_4$ with an average particle size of about 14, 27, 40 and 106 nm, respectively (Fig. 2a). The increase in the T_N with increasing particle size has also been observed in $NiFe_2O_4$ [22].

From the comparison of our present data with the data of O'Neill *et al*. [29], it follows that the T_N values of 632, 636, 643 and 648 K, characterizing the magnetic disorder–order transition in $MgFe_2O_4$ with four different particle sizes, correspond to samples with the degree of inversion of 0.870(8), 0.879(1), 0.893(4) and 0.903(7), respectively (Fig. 2b). This indicates that the nonequilibrium cation distribution in $MgFe_2O_4$ resulting from the mechanical treatment is reversible, i.e., during the annealing process, it relaxes towards its equilibrium configuration (λ=0.90 [21]).

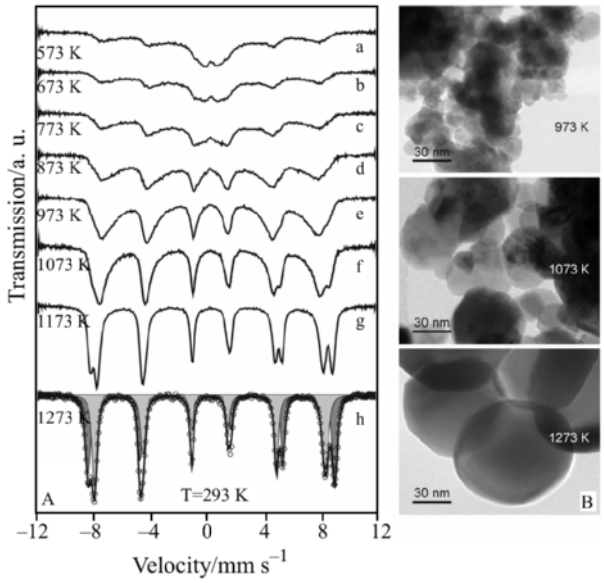

Fig. 3 A – Room-temperature Mössbauer spectra of mechanosynthesized $NiFe_2O_4$ after annealing at various temperatures for 30 min. B – TEM bright-field images of mechanosynthesized $NiFe_2O_4$ after annealing at 973, 1073 and 1273 K reveal different particle sizes

Thermal stability and particle size dependent magnetic properties of mechanosynthesized spinel ferrite

To determine the range of the thermal stability of mechanosynthesized $NiFe_2O_4$, its response to changes in temperature was followed by ^{57}Fe Mössbauer spectroscopy. Figure 3 shows the room-temperature Mössbauer spectra of the mechanosynthesized material taken after annealing at various temperatures. It was observed that in the temperature range 293–673 K, the spectra, dominated by a superparamagnetic doublet characteristic of nanoscale magnetic particles, remain unchanged (compare Figs 3a and b). This demonstrates that the range of the thermal stability of the mechanosynthesized product extends up to 673 K. However, at T>673 K, the superparamagnetic doublet gradually vanishes because of particle growth of the spinel phase. Simultaneously, the sextet structure, typical of the long-range ferrimagnetic state, develops because of the thermally induced changes in the spin configuration. The spectrum of the mechanosynthesized $NiFe_2O_4$ after annealing at 1273 K (Fig. 3h) consists of two sextets with the average magnetic hyperfine fields $B_{(A)}$=49.21(3) T and $B_{[B]}$=52.90(2) T, which are well comparable with those of the bulk material [22]. The quantitative evaluation of this spectrum revealed that the annealed sample exhibits the fully inverse spinel structure (λ=1) with a Néel-type collinear spin alignment of $(Fe\uparrow)[NiFe\downarrow]O_4$. This is in contrast to the mechanosynthesized $NiFe_2O_4$ nanoparticles before annealing, which were found to exhibit the so-called

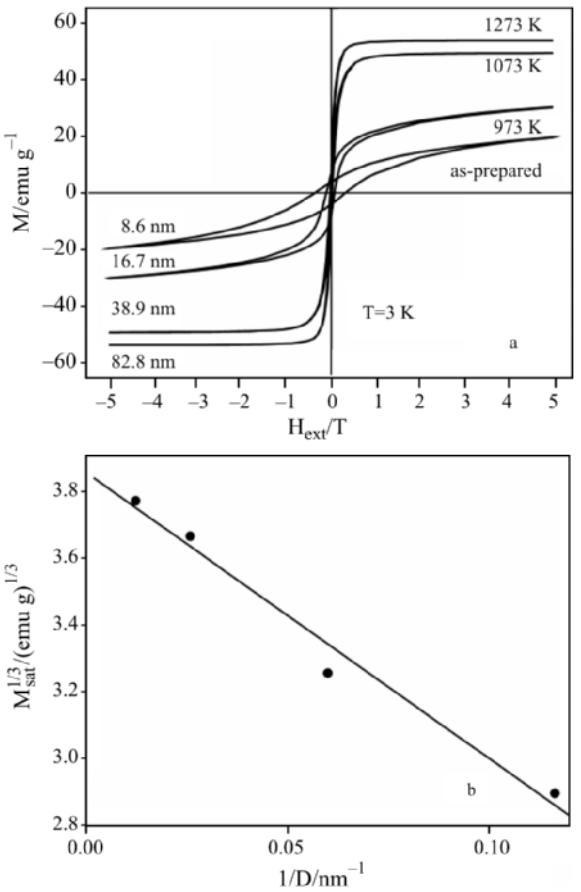

Fig. 4 a – Hysteresis loops measured at 3 K for mechanosynthesized and subsequently annealed $NiFe_2O_4$ samples. The annealing temperatures and corresponding particle sizes are shown in the figure. b – $M_{sat}^{1/3}$ *vs*. $1/D$ plot, where M_{sat} is the saturation magnetization and D is the particle diameter

Table 1 Average particle diameter (D), saturation magnetization (M_{sat}) and coercivity (H_C) for mechanosynthesized and subsequently annealed $NiFe_2O_4$

Sample	D/nm[a]	M_{sat}/emu g^{-1} [b]	H_C/T
Mechanosynthesized $NiFe_2O_4$	8.6(3)	24.35	0.351
$NiFe_2O_4$ annealed at 973 K	16.7(4)	34.55	0.107
$NiFe_2O_4$ annealed at 1073 K	38.9(8)	49.22	0.024
$NiFe_2O_4$ annealed at 1273 K	82.8(9)	53.62	0.013

[a]Values of the average crystallite size determined by XRD. [b]Values of the saturation magnetization at T=3 K obtained by linear extrapolation of the high-field region (H_{ext}>3.5 T) of the $M(H_{ext})$ curves to infinite field

core–shell structure consisting of a ferrimagnetically ordered inner core surrounded by a surface shell with a nonequilibrium cation distribution and a canted spin arrangement [25].

SQUID measurements have revealed that the saturation magnetization (M_{sat}) of the mechanosynthesized $NiFe_2O_4$ increases with increasing annealing temperature, i.e., with increasing particle size (Fig. 4a and Table 1). After annealing at 1273 K, it reaches the value of M_{sat}=53.6 emu g^{-1}, which is close to the bulk one (52.9 emu g^{-1} [22]). Increasing annealing temperatures also result in a continuous decrease of coercivity from H_C=0.351 T (before annealing) to H_C=0.013 T for the sample after annealing at 1273 K. Thus, on heating, the mechanosynthesized $NiFe_2O_4$ has relaxed to a magnetic state that is similar to the bulk one.

The thermally induced increase of the saturation magnetization (Fig. 4a) suggests that the surface-to-volume fraction in the mechanosynthesized material decreases with increasing annealing temperature. Assuming a spherical shape of mechanosynthesized and subsequently annealed $NiFe_2O_4$ particles, in the following, we will estimate the thickness (t) of the surface shell surrounding the particle core using the experimentally determined D and M_{sat} values of the sample annealed at various temperatures (Table 1). Assuming that t is independent of D and that the shell is magnetically 'dead' (M=0) [30], the variation of M_{sat} with D will then be described by

$$M_{sat}=M_{sat0}(D-2t)^3/D^3$$

or

$$M_{sat}^{1/3} = M_{sat0}^{1/3}(1-2t/D)$$

where M_{sat0} is the saturation magnetization of a ferrimagnetically ordered core of $NiFe_2O_4$ nanoparticles.

As can be seen in Fig. 4b, the present experimental data $M_{sat}^{1/3}$ and $1/D$ indeed show a good linear relationship. Note that the intercept at $1/D$=0 and the slope of the straight line correspond to $M_{sat0}^{1/3}$ and $2tM_{sat0}^{1/3}$, respectively. From a linear fit to the data points, the saturation magnetization of the particle core and the thickness of the surface shell were estimated to be M_{sat0}≈57.2 emu g^{-1} and t≈1.1 nm, respectively. M_{sat0} thus obtained is close to the value of the saturation magnetization measured for bulk $NiFe_2O_4$ [22]. The value of the shell thickness of mechanosynthesized $NiFe_2O_4$ nanoparticles is comparable to that obtained from magnetic measurements on mechanosynthesized $MnFe_2O_4$ (0.91 nm) [13], and ball-milled $NiFe_2O_4$ (0.88 nm) [31], as well as from Mössbauer experiments on nanosized $CoFe_2O_4$ (1.0–1.6 nm) [32] and mechanosynthesized $MgFe_2O_4$ (0.9 nm) [21].

Conclusions

Metastable nanocrystalline $MgFe_2O_4$ and $NiFe_2O_4$ prepared by mechanochemical route were annealed at vari-

ous temperatures to investigate the changes induced in their microstructure and magnetic properties. The thermogravimetric measurements allowed to sensitively monitor the relaxation of the mechanically induced cation distribution in $MgFe_2O_4$ towards its equilibrium configuration (λ=0.90). ^{57}Fe Mössbauer spectroscopic measurements revealed that the range of the thermal stability of the mechanosynthesized $NiFe_2O_4$ extends up to about 673 K. The study also demonstrates that one can tailor the magnetic properties of mechanochemically prepared particles by suitably controlling their size. The Néel temperature of $MgFe_2O_4$ was found to increase with increasing particle size from about 632 K at 14 nm to 648 K at 106 nm. Increasing particle size induced by annealing at elevated temperatures brings about an increase in the saturation magnetization of mechanosynthesized $NiFe_2O_4$ to a value of M_{sat}= 53.6 emu g^{-1} which is close to the bulk one. Assuming the core–shell structure of mechanosynthesized nanoparticles consisting of a ferrimagnetically ordered core surrounded by a magnetically 'dead' layer at the particle surface, the thickness of the surface shell was estimated to be about 1.1 nm. On heating to elevated temperatures, nanoscale $MgFe_2O_4$ and $NiFe_2O_4$ prepared by mechanochemical route relax to a structural and magnetic state that is similar to that of their bulk counterparts.

Acknowledgements

The present work was supported by the Deutsche Forschungsgemeinschaft. Partial support by the Grant Agency of the Ministry of Education of the Slovak Republic and of the Slovak Academy of Sciences (Grant 2/5146/25) and by the Alexander von Humboldt Foundation is gratefully acknowledged.

References

1 C. Zhou, T. C. Schulthess and D. P. Landau, J. Appl. Phys., 99 (2006) 08H906.
2 Z. L. Wang, Y. Liu and Z. Zhang, Handbook of Nanophase and Nanostructured Materials, Vol. 3, Kluwer Academic/Plenum Publishers, New York 2002.
3 M. Sugimoto, J. Am. Ceram. Soc., 82 (1999) 269.
4 M. A. Willard, L. K. Kurihara, E. E. Carpenter, S. Calvin and V. G. Harris, Int. Mater. Rev., 49 (2004) 125.
5 U. Lüders, A. Barthélémy, M. Bibes, K. Bouzehouane, S. Fusil, E. Jacquet, J.-P. Contour, J.-F. Bobo, J. Fontcuberta and A. Fert, Adv. Mater., 18 (2006) 1733.
6 V. V. Boldyrev, Russ. Chem. Rev., 75 (2006) 177.
7 Y. T. Pavlyukhin, Y. Y. Medikov and V. V. Boldyrev, J. Solid State Chem., 53 (1984) 155.
8 V. Šepelák, D. Baabe, F. J. Litterst and K. D. Becker, J. Appl. Phys., 88 (2000) 5884.
9 V. Šepelák, I. Bergmann, S. Kipp and K. D. Becker, Z. Anorg. Allg. Chem., 631 (2005) 993.
10 E. Avvakumov, M. Senna and N. Kosova, Soft Mechanochemical Synthesis: A Basis for New Chemical Technologies, Kluwer Academic Publishers, Boston 2001.
11 V. Šepelák, U. Steinike, D. C. Uecker, S. Wissmann and K. D. Becker, J. Solid State Chem., 135 (1998) 52.
12 G. F. Goya, H. R. Rechenberg, M. Chen and W. B. Yelon, J. Appl. Phys., 87 (2000) 8005.
13 M. Muroi, R. Street, P. G. McCormick and J. Amighian, Phys. Rev. B, 63 (2001) 184414.
14 W. Kim and F. Saito, Powder Technol., 114 (2001) 12.
15 V. G. Harris, D. J. Fatemi, J. O. Cross, E. E. Carpenter, V. M. Browning, J. P. Kirkland, A. Mohan and G. J. Long, J. Appl. Phys., 94 (2003) 496.
16 N. Guigue-Millot, S. Begin-Colin, Y. Champion, M. J. Hytch, G. Le Caër and P. Perriat, J. Solid State Chem., 170 (2003) 30.
17 E. Manova, B. Kunev, D. Paneva, I. Mitov, L. Petrov, C. Estournès, C. D'Orléans, J.-L. Rehspringer and M. Kurmoo, Chem. Mater., 16 (2004) 5689.
18 S. K. Pradhan, S. Bid, M. Gateshki and V. Petkov, Mater. Chem. Phys., 93 (2005) 224.
19 P. Osmokrović, Č. Jovalekić, D. Manojlović and M. B. Pavlović, J. Optoelectron. Adv. Mater., 8 (2006) 312.
20 S. Dasgupta, K. B. Kim, J. Ellrich, J. Eckert and I. Manna, J. Alloys Compd., 424 (2006) 13.
21 V. Šepelák, A. Feldhoff, P. Heitjans, F. Krumeich, D. Menzel, F. J. Litterst, I. Bergmann and K. D. Becker, Chem. Mater., 18 (2006) 3057.
22 V. Šepelák, D. Baabe, D. Mienert, D. Schultze, F. Krumeich, F. J. Litterst and K. D. Becker, J. Magn. Magn. Mater., 257 (2003) 377.
23 V. Šepelák, U. Steinike, D. C. Uecker, R. Trettin, S. Wissmann and K. D. Becker, Solid State Ionics, 101–103 (1997) 1343.
24 V. Šepelák, M. Menzel, I. Bergmann, M. Wiebcke, F. Krumeich and K. D. Becker, J. Magn. Magn. Mater., 272–276 (2004) 1616.
25 V. Šepelák, I. Bergmann, A. Feldhoff, P. Heitjans, F. J. Litterst and K. D. Becker, Hyperfine Interact., 165 (2005) 81.
26 K. Lagarec and D. G. Rancourt, Recoil - Mössbauer Spectral Analysis Software for Windows, Version 1.02, Department of Physics, University of Ottawa, Ottawa, ON 1998.
27 G. A. Sawatzky, F. Van Der Woude and A. H. Morrish, Phys. Rev., 183 (1969) 383.
28 W. Kraus and G. Nolze, PowderCell for Windows, Version 2.4, Federal Institute for Materials Research and Testing, Berlin, Germany 2000.
29 H. St. C. O'Neill, H. Annersten and D. Virgo, Am. Miner., 77 (1992) 725.
30 M. George, A. M. John, S. S. Nair, P. A. Joy and M. R. Anantharaman, J. Magn. Magn. Mater., 302 (2006) 190.
31 Y. D. Zhang, S. H. Ge, H. Zhang, S. Hui, J. I. Budnick, W. A. Hines, M. J. Yacaman and M. Miki, J. Appl. Phys., 95 (2004) 7130.
32 K. Haneda and A. H. Morrish, J. Appl. Phys., 63 (1988) 4258.

DOI: 10.1007/s10973-007-8481-1